lubricants

MDPI

Article

High-Temperature Friction and Wear Behavior of Nickel-Alloy Matrix Composites with the Addition of Molybdate

Jinming Zhen [1,*], Congcong Zhen [2], Yunxiang Han [1], Lin Yuan [1], Liwei Yang [1], Tianqi Yang [1] and Shuo Guo [1]

[1] College of Materials Science and Engineering, Liaocheng University, Liaocheng 252059, China; hanyxd@163.com (Y.H.); 19111912571@163.com (L.Y.); 15966080229@163.com (L.Y.); 15806768126@163.com (T.Y.); xtbest021130@163.com (S.G.)

[2] Zibo Vocational Institute, Zibo 255314, China; zcc.cool@163.com

* Correspondence: zhenjinming@lcu.edu.cn; Tel.: +86-13563040259

Abstract: To improve the tribological characteristics of materials employed in spatial mechanisms, there is a significant requirement to develop solid lubricating composites with superior performance. This study investigates the tribological characteristics of composites consisting of a nickel matrix combined with silver molybdate and barium molybdate. The experimental analysis focuses on evaluating the tribological behaviors of these composites from 25 °C to 800 °C. The findings indicate that the combined application of silver molybdate and barium molybdate resulted in enhanced self-lubricating properties of the composites, particularly at temperatures over 400 °C. The inclusion of both silver molybdate and barium molybdate in the composite resulted in the achievement of a low friction coefficient (0.34–0.5), as well as a wear rate ranging from 0.47 to 1.25 × 10^{-4} mm^3 $N^{-1}m^{-1}$, within the temperature range of 400 to 800 °C. Furthermore, an analysis was conducted to examine the wear processes of the composites at various sliding temperatures. This analysis was based on the evaluation of the chemical composition and morphologies of the sliding surfaces, which were verified by scanning electron microscopy (SEM), energy-dispersive X-ray spectroscopy (EDS), and Raman spectroscopy.

Keywords: nickel-alloy matrix composite; molybdate; dry sliding; high-temperature tribology

check for updates

Citation: Zhen, J.; Zhen, C.; Han, Y.; Yuan, L.; Yang, L.; Yang, T.; Guo, S. High-Temperature Friction and Wear Behavior of Nickel-Alloy Matrix Composites with the Addition of Molybdate. *Lubricants* **2023**, *11*, 516. https://doi.org/10.3390/lubricants11120516

Received: 2 November 2023
Revised: 30 November 2023
Accepted: 4 December 2023
Published: 7 December 2023

Copyright: © 2023 by the authors. Licensee MDPI, Basel, Switzerland. This article is an open access article distributed under the terms and conditions of the Creative Commons Attribution (CC BY) license (https://creativecommons.org/licenses/by/4.0/).

1. Introduction

High-temperature solid lubricant composites have become increasingly necessary for extreme operating environments (high vacuum, high radiation, and high temperatures) due to the rapid development of advanced manufacturing systems (aerospace, nuclear, automobile industries, etc.) [1–5]. In the aforementioned systems, a variety of moving components (rolling and sliding bearings as well as gears) are subjected to intense working circumstances characterized by temperatures above 400 °C, significant speeds and loads, corrosive surroundings, and vacuum environments [6–8]. In such scenarios, traditional liquid lubricants cannot meet the requisite performance requirements, particularly when operating at temperatures over 350 °C. This limitation arises from issues such as evaporation, decomposition, coking, and sealing [2]. Instead, solid-lubricating materials show great potential to fulfill the friction-reduction and wear-resistance needs of the moving elements in these service environments [9,10]. It has been reported that one of the most famous materials, PS coatings, has proven successful in many applications. The PS coatings employ silver and fluoride eutectic (CaF_2/BaF_2) as solid lubricants and oxide/carbide as a hardener, and results show that due to the synergistic effect of low-to-moderate lubricant silver and moderate-to-high lubricant CaF_2/BaF_2, the materials exhibit excellent lubricating properties at broad temperatures. Furthermore, Zhu et al. and Shi et al. [11–17] have conducted research on the development of Ni_3Al/NiAl matrix composites that incorporate a combination of solid lubricants (Ag, BaF_2/CaF_2, Ti_3SiC_2, WS_2, hBN, etc.). These composites have demonstrated excellent self-lubricating properties across a broad temperature range from

room temperature to 800 °C, and this can be attributed to the synergistic lubricating effect of the added solid lubricants and the formation of an oxidation protection film on the worn surface, as discussed in previous studies. Ripoll et al. discovered that the enhanced lubricating capabilities of the NiCrBSi-Ag-MoS_2 coating can be attributed to the combined presence of Cr_xS_y and Ag at temperatures below 400 °C. Moreover, at temperatures of 600 and 800 °C, the formation of a glazed tribolayer containing Cr_xS_y, MoO_3, and a silver molybdate phase was identified as a contributing factor to the improved performance [18]. In addition, there has been substantial research conducted on ceramic matrix self-lubricating composites. Dry sliding tests on Al_2O_3/BN and Al_2O_3/MoS_2 coatings were part of the experimental study. The results indicated that the incorporation of solid lubricants such as BN and MoS_2 led to enhanced tribological characteristics of the samples, particularly when subjected to low-load friction conditions of 5 and 10 N [19]. According to Zhao et al., the synthesis Al_2O_3/Ag coating had a reduced wear rate compared to the Al_2O_3/Ag coating, attributed to its dense microstructure and superior mechanical characteristics [20]. In their study, Bi et al. conducted a systematic investigation into the impact of various solid lubricants, including graphite, Mo, BaF_2/CaF_2, Ag, CaF_2, and MoS_2, on the frictional behavior of ZrO_2 (Y_2O_3) matrix composites at high temperatures, and their research demonstrated that the combined lubricating effect of low-temperature lubricants, such as Ag, graphite, and MoS_2, along with high-temperature lubricants like CaF_2, BaF_2/CaF_2, and molybdate, played a significant role in reducing friction and wear across a wide temperature range [21–23].

In addition to the above-mentioned direct addition of solid lubricants, the formation of in situ oxide phases on the deteriorated surface is also an effective way of achieving this objective. Based on this, several researchers have devoted increased attention to the development of solid lubricating materials by the direct addition or in situ formation of double metal oxide phases (DMO) [24–26]. The Air Force Research Laboratory has successfully created a series of adaptable solid-lubricating nanocomposite coatings, commonly referred to as "chameleon" coatings. These coatings have demonstrated exceptional lubricating capabilities in both air and vacuum environments, ranging from temperatures of 25 to 800 °C and even up to 1000 °C. The incorporation of Ag/Au, dichalcogenides (WS_2, MoS_2), and carbon phases has been utilized in these materials for the purpose of achieving low to moderate lubrication. On the other hand, oxides and DMO have been shown to offer minimal friction at elevated temperatures [27]. Zhu et al. reported that Ni_3Al alloy-Ag exhibits favorable self-lubricating performance as a result of the effect of Ag and the in situ formation of a lubricous coating film composed of Ag_2MoO_4 [28]. Wan et al. reported that the enhanced wear resistance of a nickel-based coating, including TiO_2-ZnO-MoO_3, was attributed to the existence of binary oxides as well as ternary oxides, such as A-TiO_2, R-TiO_2, $ZnMoO_4$, Zn_2TiO_4, etc. [29]. Zhou et al. reported that the formation of $AgCrO_2$ and $BaCrO_4$ can enhance the lubricating and abrasion resistance properties of Ag-BaF_2/CaF_2-Cr_3C_2-NiCr coatings at moderate to high temperatures [30]. In a similar vein, it has been observed that the wear characteristics of YSZ coatings incorporating Ag and Ag_2MoO_4 nanoparticles are influenced by the presence of liquid lubrication and the creation of a stable tribofilm. These factors collectively lead to the notable longevity of the lubricating performance [31]. Yang et al. conducted an investigation on the frictional behaviors of nickel-alloy matrix composites from 25 °C to 800/900 °C and found that the presence of silver, silver molybdate, and nickel oxide exhibited a synergistic effect that led to reduced friction and wear in the nickel-alloy matrix composites [32–35]. Furthermore, it has been demonstrated that the tribological characteristics of NiAl-MoO_3/CuO are influenced by the presence of $NiMoO_4$, which effectively reduces both the friction coefficient and wear rate at elevated temperatures [36].

It has been reported that the in situ formation of double metal oxide phases could increase the frictional properties at high temperatures, such as Ag_2MoO_4, $BaMoO_4$, $AgVO_3$, $AgTaO_3$, etc. [3,24,27,37]. To further investigate the lubricating behavior of the double metal oxide and get a high-performance solid lubricating composite, in this work, the nickel-alloy matrix composites with silver molybdate/barium molybdate composites were

fabricated by the hot-pressing sintering method, and their frictional behaviors in air at temperatures ranging from 25 to 800 °C were investigated. This work also aimed to fabricate high-performance solid lubricant composites and further investigate the influence of molybdate on the frictional behavior of the composite. The wear mechanism was analyzed by considering the properties and tribochemical reactions of the contact surfaces. The results of this study will provide theoretical guidance and technical support for solving the practical application problems of broad-temperature lubrication and wear resistance in sophisticated equipment.

2. Experimental Part

2.1. Materials

In the present study, three composites with distinct compositions have been produced using the hot-pressed sintering technique; their compositional constitutions are listed in Table 1. The processing parameters have been described elsewhere [38].

Table 1. Detailed composition of the composites (wt. %).

Composites	NiCrMoTiAl	Silver Molybdate	Barium Molybdate
NA	90	10	
NB	90		10
NAB	80	10	10

2.2. Tribological Performance Tests

The present study involved the execution of ball-on-disk dry sliding wear experiments (HT-1000 high-temperature surface tester, Zhongke Kaihua Corporation in Lanzhou, China). The primary objective of these tests was to examine the frictional characteristics exhibited by the nickel-alloy matrix composites. As counterpart materials, commercially available Si_3N_4 ceramic balls were used, and the tribological tests were conducted under laboratory ambient conditions, as depicted in Figure 1. The friction tests were conducted under a wide temperature range of 25 to 800 °C for 30 min with a load of 5 N and a sliding speed of 1 m/s. The coefficient of friction (COF) was systematically measured and subsequently recorded in an automated manner during the process of sliding. The resulting data presented the average value derived from the original dataset. The wear tracks were subjected to measurement using a contact surface profilometer. This particular method was employed in order to effectively characterize the alterations in wear volume subsequent to the testing process. Furthermore, the wear rate (W) was determined through the utilization of a specific formula.

$$W = \frac{V}{F \cdot \mathrm{L}} \tag{1}$$

where V is the wear volume (mm^3), F is the applied load (N), and L is the sliding distance (m).

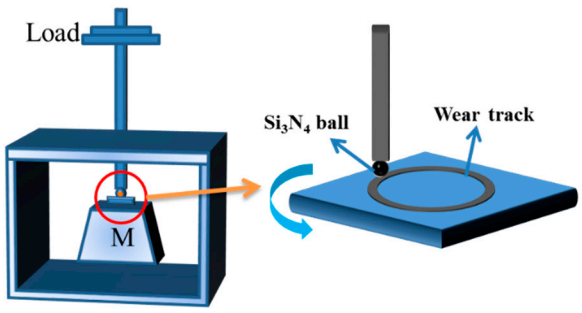


Figure 1. Schematic diagram of a friction testing machine.

2.3. Characterization

The Contourgraph (SuperView W3, Chotest Technology Inc. in Shenzhen, China.) was employed as a tool to effectively analyze and describe the intricate three-dimensional morphology of the worn surface. The worn composites were subjected to a comprehensive characterization using advanced analytical techniques, including the Raman spectrometer (Renishaw inVia Reflex, operating at a wavelength of 532 nm) and a scanning electron microscope (FE-SEM, JSM5600LV) equipped with an energy-dispersive spectrometer (EDS). These analytical tools were employed to investigate the alterations in morphological features and the surface compositions of the worn composites.

3. Results and Discussion

3.1. Friction and Wear Performance Test

Figures 2–5 depict the variations in COF, wear rates, and three-dimensional morphologies of the wear tracks for the composites from 25 to 800 °C. The significance of molybdate in enhancing the tribological characteristics of composites has been established. However, it is crucial to note that the lubricating properties and wear-reducing effects of molybdate are contingent upon the temperature at which testing is conducted. The NAB composites, in general, exhibit commendable tribological performance. Notably, when testing temperatures surpass 400 °C, these composites indicate comparatively low COFs and wear rates. This beneficial result can be attributed to the elevated concentration of solid lubricant present within the composites.

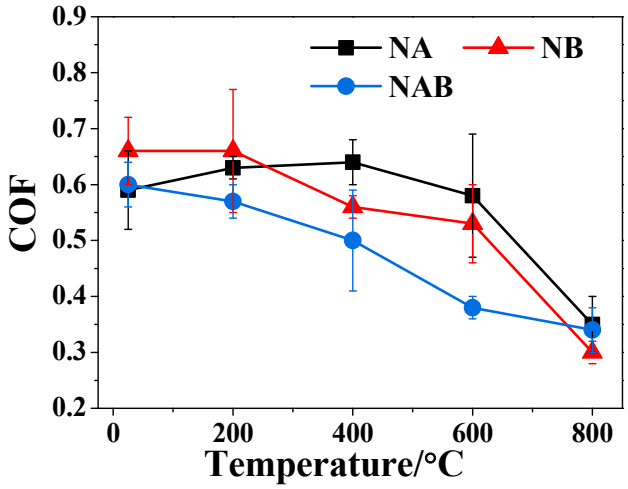


Figure 2. Friction coefficients vs. testing temperatures of nickel-alloy composites.

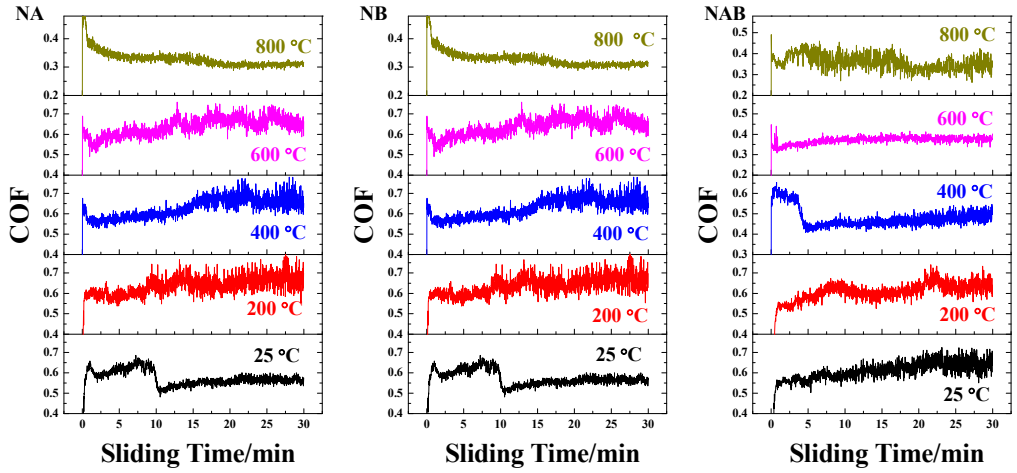


Figure 3. Typical friction curve of the three composites at different testing temperatures.

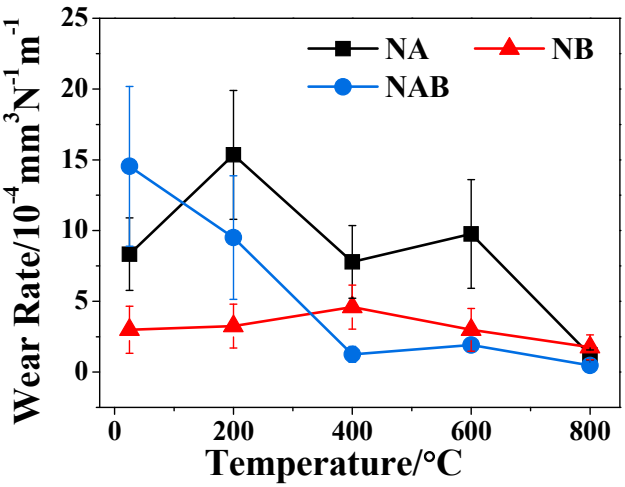


Figure 4. The wear rate of the three composites at different testing temperatures.

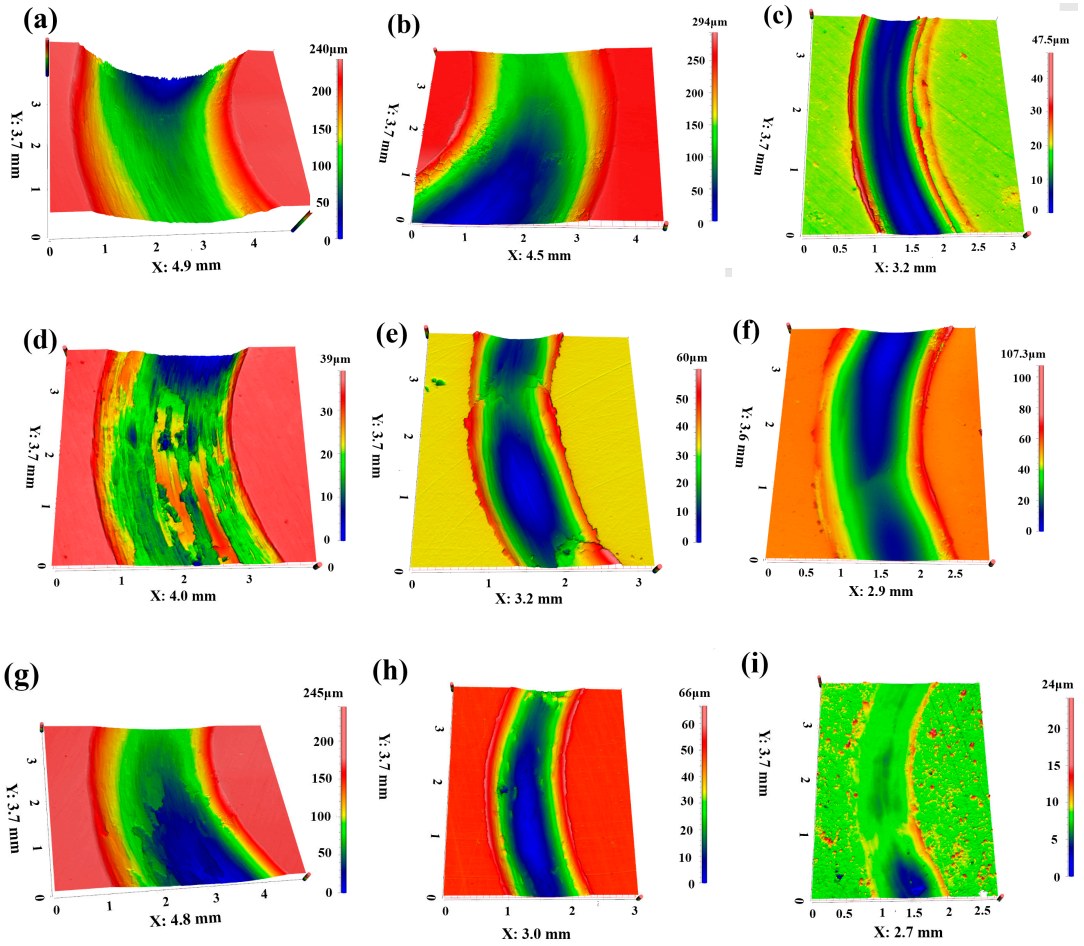


Figure 5. Three-dimensional morphologies of the worn surface for nickel-alloy matrix composites at different testing temperatures: (**a**) NA25 °C, (**b**) NA600 °C, (**c**) NA800 °C; (**d**) NB25 °C, (**e**) NB600 °C, (**f**) NB800 °C; (**g**) NAB25 °C, (**h**) NAB600 °C, and (**i**) NAB800 °C.

Figure 2 illustrates the average COF values of the three composites from 25 to 800 °C under ambient air conditions. The observed changes in the characteristics of the COFs across the three composites exhibit a remarkable similarity in response to variations in testing temperature. The COF exhibits a consistent downward trend as the temperature rises from 25 to 800 °C for both NB (from 0.66 to 0.3) and NAB (from 0.6 to 0.34) composites.

For NA composites, the value increases slightly from 25 to 400 °C (from 0.59 to 0.64) and then decreases to the minimum one at 800 °C (0.35). The impact of molybdate content on the frictional behavior of composites is found to be weak at 25 °C, 200 °C, and 800 °C. However, within the temperature range of 400 to 600 °C, NAB exhibits the lowest value (0.50 at 400 °C and 0.38 at 600 °C), followed by NB (0.56 at 400 °C and 0.53 at 600 °C) and NA (0.64 at 400 °C and 0.58 at 600 °C) composites.

The typical friction coefficient curves of nickel-alloy matrix composites with sliding time at various testing temperatures are given in Figure 3, respectively. The trends of friction coefficients under different aging durations are roughly the same: the friction coefficients were more varied in the running stage, while the value in the steady wear stage became smooth, suggesting that the stable tribofilm developed on the worn surface.

The wear rates of the composites in a temperature range of 25–800 °C are shown in Figure 4. The wear rate for the NB composite exhibits a consistent and relatively low range of 1.75–4.59 $\times$ 10^{-4} $mm^3N^{-1}m^{-1}$ from 25 to 800 °C. Conversely, the value of NA initially increases from 25 to 200 °C, reaching its highest value at 200 °C, indicating poor wear resistance at this temperature. However, as the testing temperature continues to rise, the value gradually decreases as a whole. This reduction in wear rate can be attributed to the formation of a lubricating oxide layer. Notably, at 800 °C, the NA composite demonstrates the lowest wear rate among all temperatures, measuring at 1.21 $\times$ 10^{-4} $mm^3N^{-1}m^{-1}$. In a comparative analysis, as the temperature rises from 25 to 400 °C, it has been observed that the wear rates of composite NAB exhibit a significant decrease from 14.54 $\times$ 10^{-4} $mm^3N^{-1}m^{-1}$ to 1.25 $\times$ 10^{-4} $mm^3N^{-1}m^{-1}$. Subsequently, these wear rates fluctuate slightly within a temperature range of 600–800 °C.

The wear resistance of the composite material can also be observed and evaluated through the analysis of its three-dimensional morphologies, as depicted in Figure 5. Clearly, the worn tracks are wide and deep for composites of NA and NAB at 25 °C (Figure 5a,g). We also found that large delamination appeared on the worn surface, while the wear track was shallow and some tribofilm formed on it for the NB composite (Figure 5d). Comparatively, composites NB and NAB exhibit narrow and shallow wear tracks at 600 °C (Figure 5e,h), and the worn surface is smooth, which indicates that the effective lubricating layer formed on it. As for composite NA, the worn surface characteristic is similar to that at 25 °C (Figure 5d). At 800 °C, all three composites present a narrow and shallow wear track (Figure 5c,f,i), and the morphologies of the worn surface are smooth, indicating that the presence of an oxidative lubricating film contributes to the reduction in friction and wear.

3.2. Worn Surface Analysis

Figures 6–12 show the typical SEM images of the worn surface, wear debris for the three nickel-alloy matrix composites, and the worn surface for the Si_3N_4 ceramic ball in the temperature range of 25–800 °C. At 25 °C, large grooves and delamination are the main characteristics of composites NA, NB, and NAB (Figures 6a, 7a and 8a). Combined with the wear debris (Figure 9a,d,g) and worn surface of the Si_3N_4 ceramic ball (Figures 10a, 11a and 12a), we can clearly see that composites NA and NB show large wear debris, and it is small for NAB. As for the worn surface of the Si_3N_4 ceramic ball, a large transfer film appeared for all three composites, and the main composition of the transfer film is nickel alloy, which peels off from the matrix. Moreover, the wear scar for NA and NAB is much larger than that of NB; this may be due to the high microhardness, which can be reflected in the three-dimensional topography (Figure 5d). Furthermore, high COFs were exhibited at 25 °C (Figure 2), and NB showed the lowest wear rate. Combined with the above results, we may indicate that the main wear mechanisms for the three composites are abrasive and fatigue wear at this temperature.

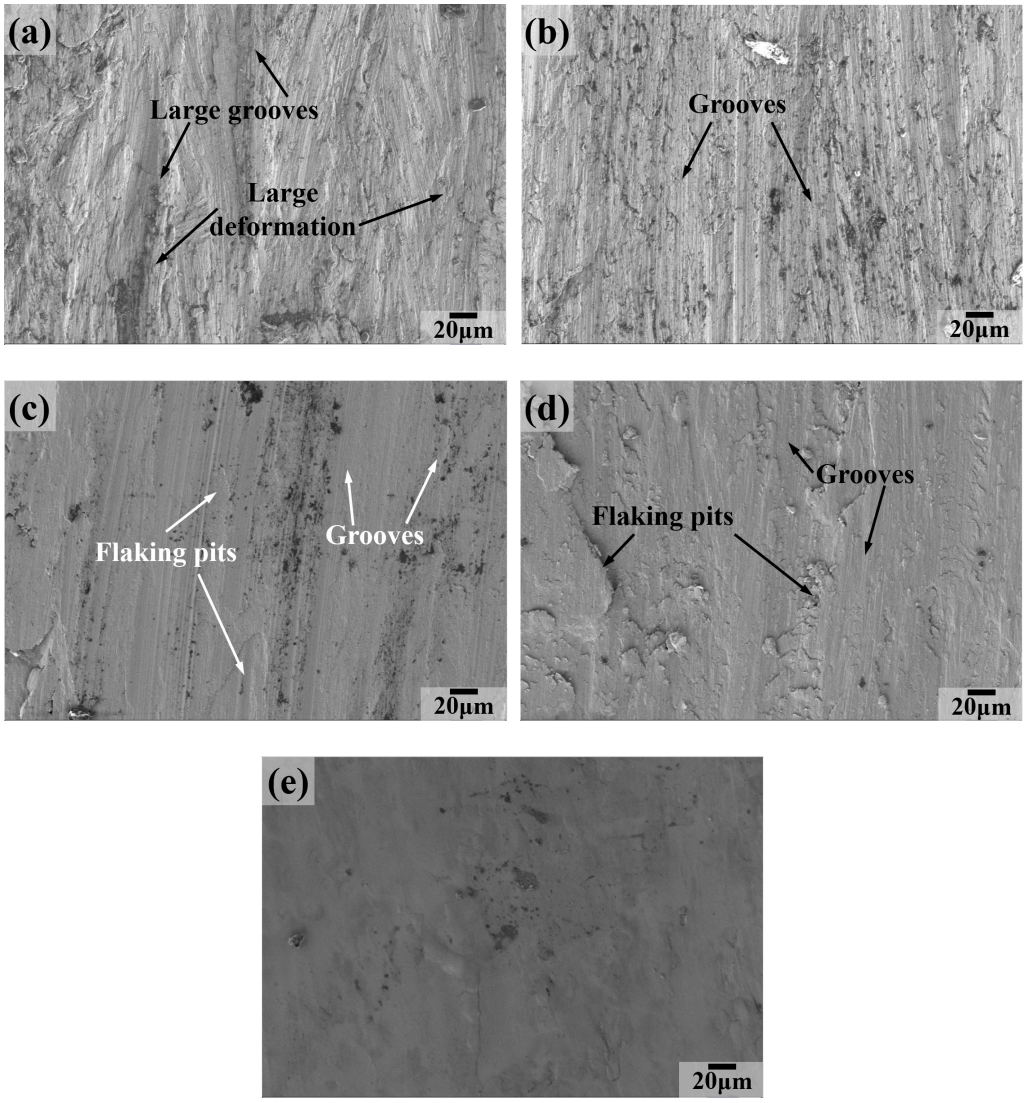


Figure 6. SEM images of the sliding surface for the NA composite at different testing temperatures: (**a**) 25 °C, (**b**) 200 °C, (**c**) 400 °C, (**d**) 600 °C, and (**e**) 800 °C.

As the temperature of the testing environment is up to 200 °C, for NA, the worn surface is characterized by grooves (Figure 6b), while for NB and NAB, delamination, cracks, or deep grooves are the main morphologies (Figures 7b and 8b) compared with those at 25 °C. The data presented in Figures 2 and 4 demonstrate a decrease in both the COF and wear rate for the composites of NB and NAB from 25 to 200 °C, while it is the opposite for the NA composite. This can also be reflected in the wear debris (Figure 9b,e,h), where the size is large for NA and NB and small for the NAB composite. Furthermore, the sliding surface of the Si_3N_4 ceramic ball (Figures 10b, 11b and 12b) also reflected that when coupled with NA and NAB, more transfer film formed on the surface than that coupled with the NB composite. The findings presented above indicate that there is a direct correlation between the size of the transfer film and the level of wear observed. This observation aligns with the aforementioned results. Overall, the primary wear mechanisms observed at 25 °C are comparable to those observed at different temperatures. These mechanisms predominantly involve abrasive wear and fatigue wear.

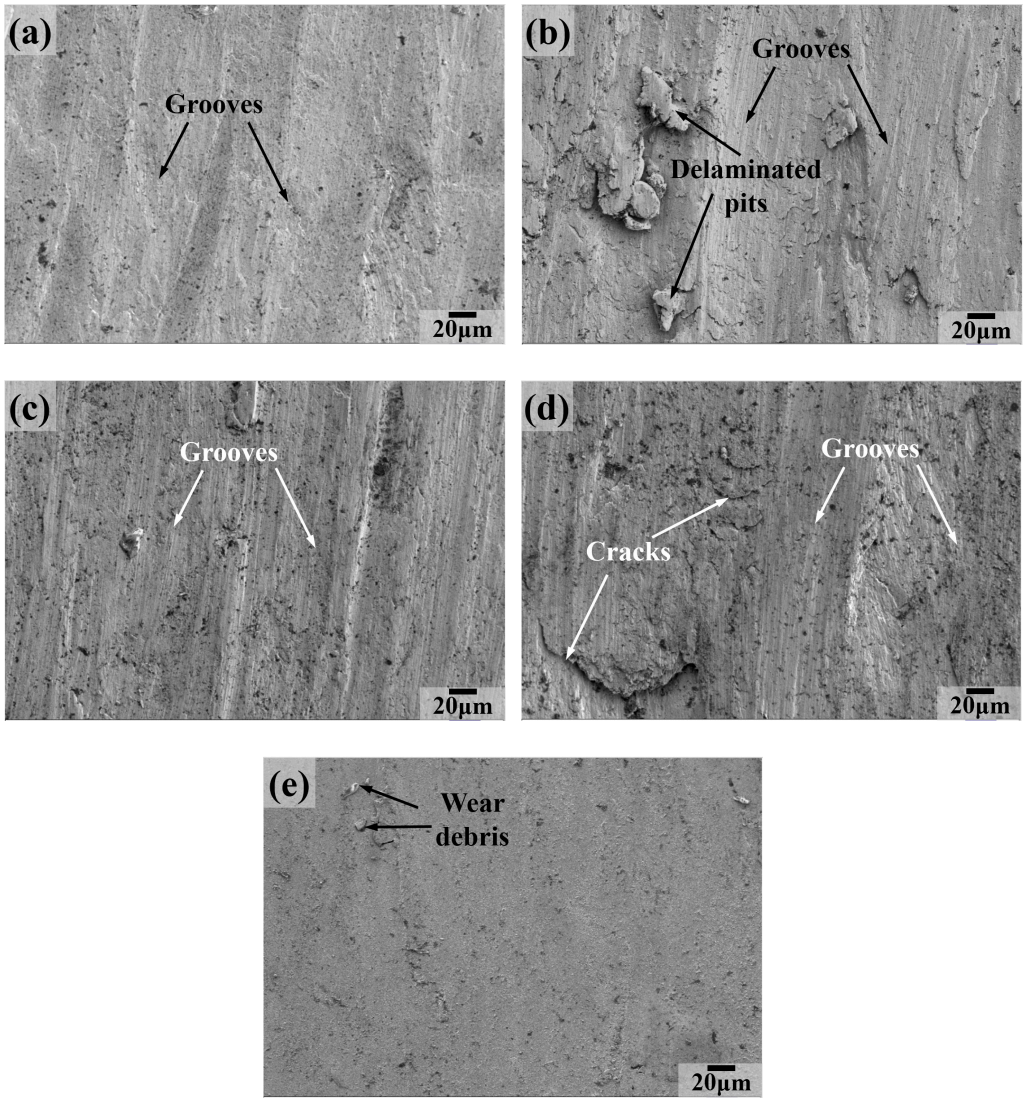


Figure 7. SEM images of the worn surface for the NB composite at different testing temperatures: (**a**) 25 °C, (**b**) 200 °C, (**c**) 400 °C, (**d**) 600 °C, and (**e**) 800 °C.

At 400 °C, a relatively smooth worn surface with small flaking pits and tiny furrows are the main features for composites of NA and NAB (Figures 6c and 8c). Instead of large grooves, as compared with those at 25 and 200 °C, for the NB composite (Figure 7c), a large groove is still the main characteristic. Combined with the worn scar for the Si_3N_4 ceramic ball, we can see that, coupled with the NB composite (Figure 11c), continuous transfer film formed on it, and the size of the worn scar is similar to that at 25 and 400 °C. In contrast, for the NA and NAB composites (Figures 10c and 12c), less transfer film forms, and the size of the worn scar is smaller than that at 25 and 200 °C, especially for NAB. The presence of an effective lubricating film on the worn surface is indicative of the observed low friction and wear in the two composites depicted in Figures 2 and 4.

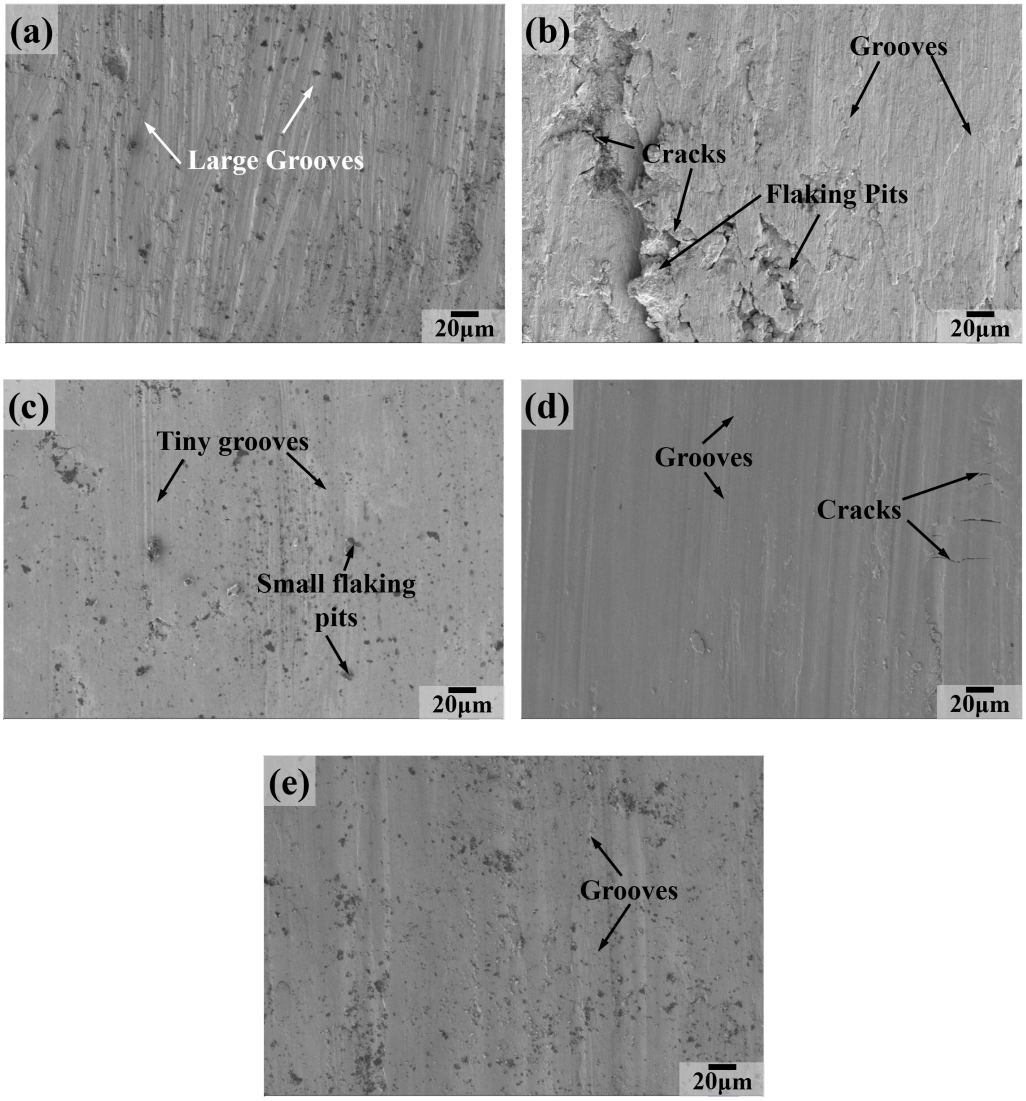


Figure 8. SEM images of the worn surface for the NAB composite at different testing temperatures: (**a**) 25 °C, (**b**) 200 °C, (**c**) 400 °C, (**d**) 600 °C, and (**e**) 800 °C.

For composites NA and NB, as the surrounding temperature increased to 600 °C, deep fissures, flaking cavities, or fractures appeared on the worn surface (Figures 6d and 7d) compared to 400 °C (Figures 6c and 7c). In this case, it is observed that the rise in temperature has a detrimental effect on the micro-hardness of the material, resulting in a decrease. Additionally, the elevated temperature facilitates surface oxidation and hastens the removal of the lubricating layer. Consequently, the lubrication process becomes ineffective, and the surface is susceptible to plowing, breakage, and peeling off oxides. This phenomenon leads to deep grooves, flaking pits, and cracks, which can also be reflected by the large wear debris and the wear scar of the ceramic ball sliding against these two composites, as shown in Figure 9c,f, Figures 10d and 11d. Therefore, NA and NB show relatively high wear rates (Figure 4), and the COFs display variability within a specific range at 600 °C (Figure 3). The worn surface for NAB (Figure 8d) becomes smooth with the exception of slight plastic deformation and tiny fractures at this testing temperature, demonstrating excellent lubricity. In addition, the worn scar of the Si_3N_4 ceramic ball reveals that the size decreases significantly, and there is little transfer film present. The findings suggest that the primary wear mechanisms for NAB are microscopic abrasive wear, while for NA and NB composites, it is abrasive/fatigue wear.

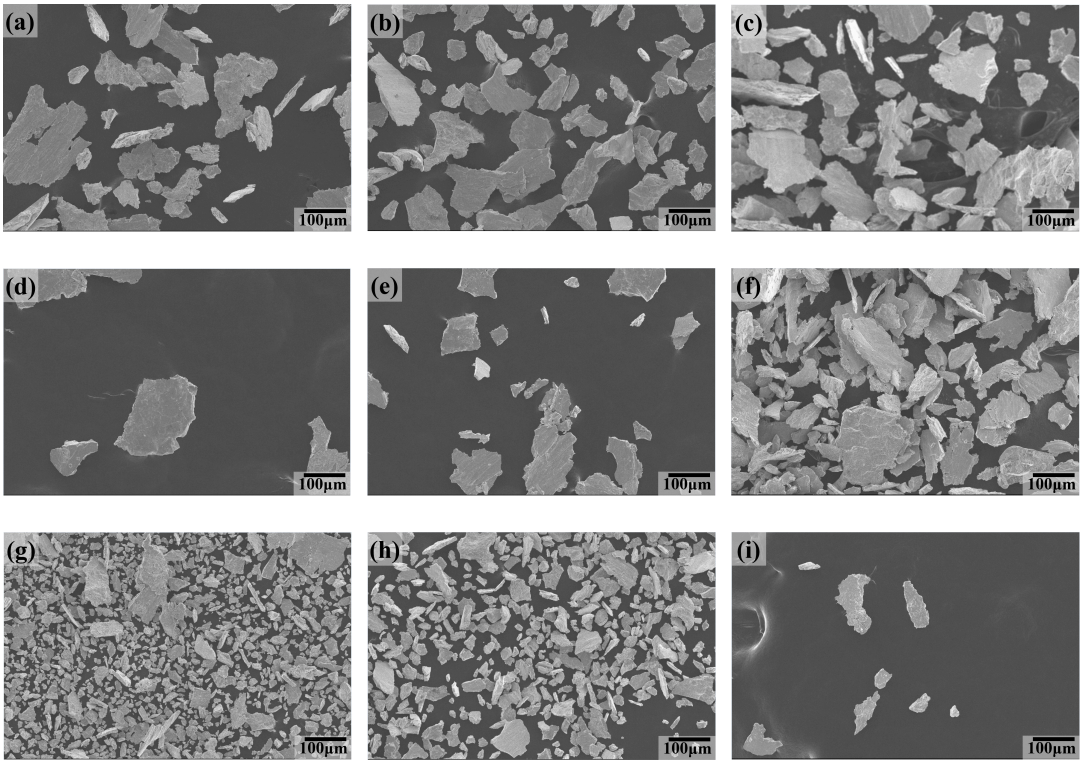


Figure 9. SEM images of the wear debris for nickel-alloy matrix composites at different testing temperatures: (**a**) NA25 °C, (**b**) NA200 °C, (**c**) NA600 °C; (**d**) NB25 °C, (**e**) NB200 °C, (**f**) NB600 °C; (**g**) NAB25 °C, (**h**) NAB200 °C, and (**i**) NAB600 °C.

As the sliding temperature increases to 800 °C, all three composites reveal a uniform glazed layer (Figures 6e, 7e and 8e) on the worn surface, and it has been demonstrated that the glazed layer can reduce friction and wear, implying that the primary wear mechanism is abrasive wear. Furthermore, the examination of the worn surface of the Si_3N_4 ceramic ball coupled with NA, NB, and NAB reveals a notable absence of a transfer film on the sliding surface (as depicted in Figures 10e, 11e and 12e). Additionally, it is observed that the size of the worn scar significantly diminishes, reaching its smallest magnitude. This is inconsistent with the friction and wear results (Figure 5) and indicates that adding silver molybdate and barium molybdate could increase the lubricating properties due to the synergistic effect.

To better comprehend the composite's wear behavior at elevated temperatures, the element distribution and the phase constituents of the worn surface were analyzed by the micro-zone Raman spectrum (Figure 13) and by SEM (with EDS) (Figures 14–16). Results indicate that the main phase constituents are $BaMoO_4$, Ag_2MoO_4, and $NiCr_2O_4$ [39–41], and the intensity of these oxides increases as the testing temperature rises from 25 to 800 °C (Figure 13c), which is consistent with the previously reported results. Furthermore, it has been shown that the oxide layer with these constituents can reduce friction and wear effectively in a tribopair system [6,28]. In addition, the SEM and EDS results also indicate that the oxygen content rises as the testing temperature increases. The relatively low wear rate of composites at 600 °C and 800 °C can therefore be attributed to the formation of a high-strength oxide layer on the worn surface. Furthermore, it can be concluded that the good lubricating performance of NAB at elevated temperatures was attributed to the synergistic lubricating effect of the molybdate compound and the in-situ-formed oxide on the worn surfaces.

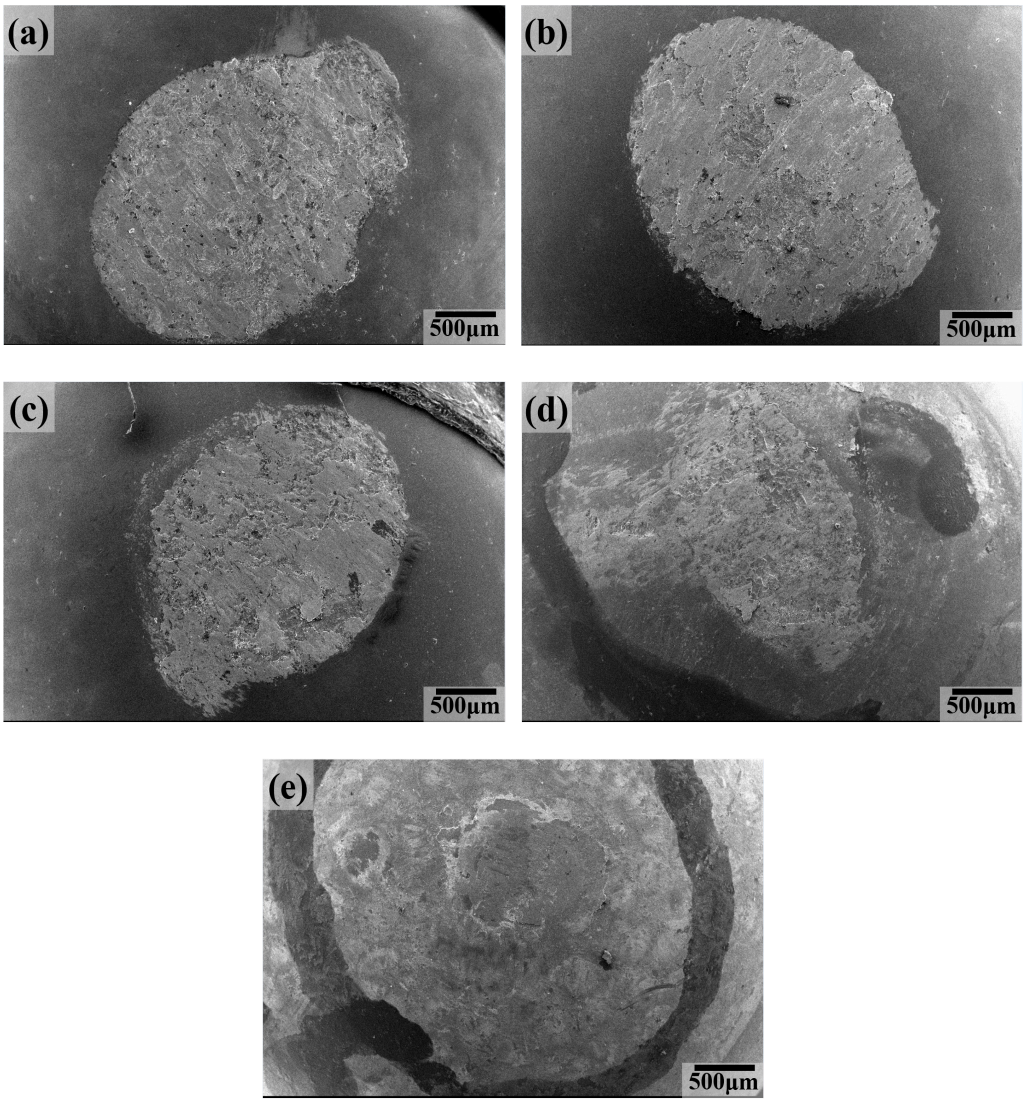


Figure 10. SEM images of the worn surface of the Si_3N_4 ceramic ball sliding against NA composite at different testing temperatures: (**a**) 25 °C, (**b**) 200 °C, (**c**) 400 °C, (**d**) 600 °C, and (**e**) 800 °C.

Based on the above-mentioned experimental results, a schematic diagram for composites tested from 25 to 800 °C was depicted, as shown in Figure 17. In conclusion, all three composites exhibited similar wear behavior under the testing conditions. From 25 to 400 °C, most parts of the tribofilm formed on the worn surface are flaking off with the wear debris during sliding contact, and a large transfer film forms on the contact surface of the Si_3N_4 ceramic ball, indicating that there is no effective lubricating film formed, so high COFs are exhibited for the three composites (Figures 2 and 3). As the testing temperature increases to 600/800 °C, the worn surface is covered with a compacted glazed layer consisting primarily of Ag_2MoO_4, $BaMoO_4$, and $NiCr_2O_4$. Furthermore, the wear scar of the Si_3N_4 ceramic ball is very small, and there is almost no transfer film on it; thus, the best lubricating property is exhibited at elevated temperatures.

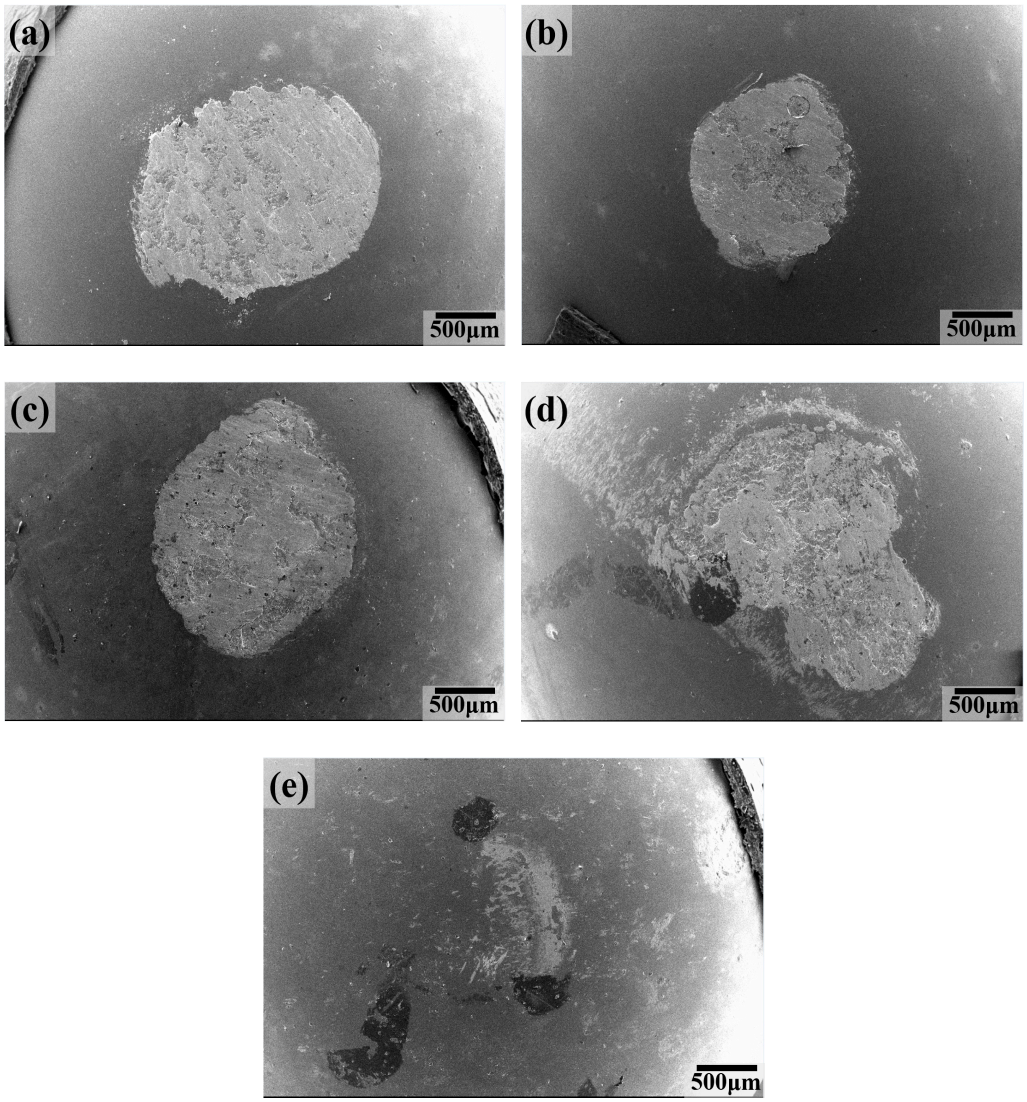


Figure 11. SEM images of the worn surface of the Si_3N_4 ceramic ball sliding against the NB composite at different testing temperatures: (**a**) 25 °C, (**b**) 200 °C, (**c**) 400 °C, (**d**) 600 °C, and (**e**) 800 °C.

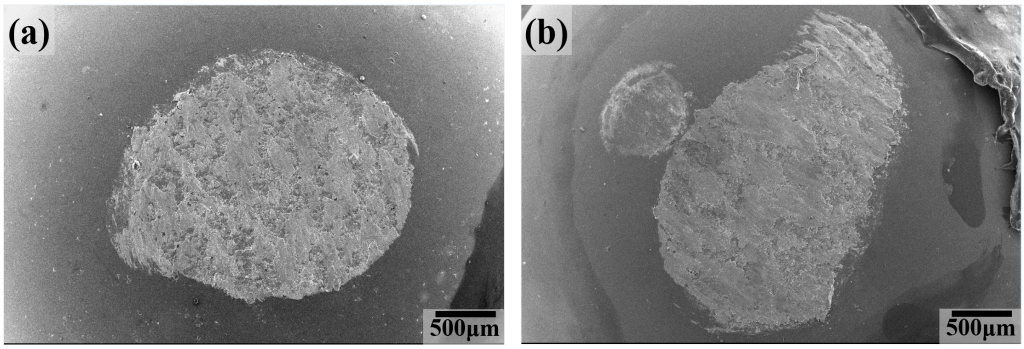


Figure 12. *Cont*.

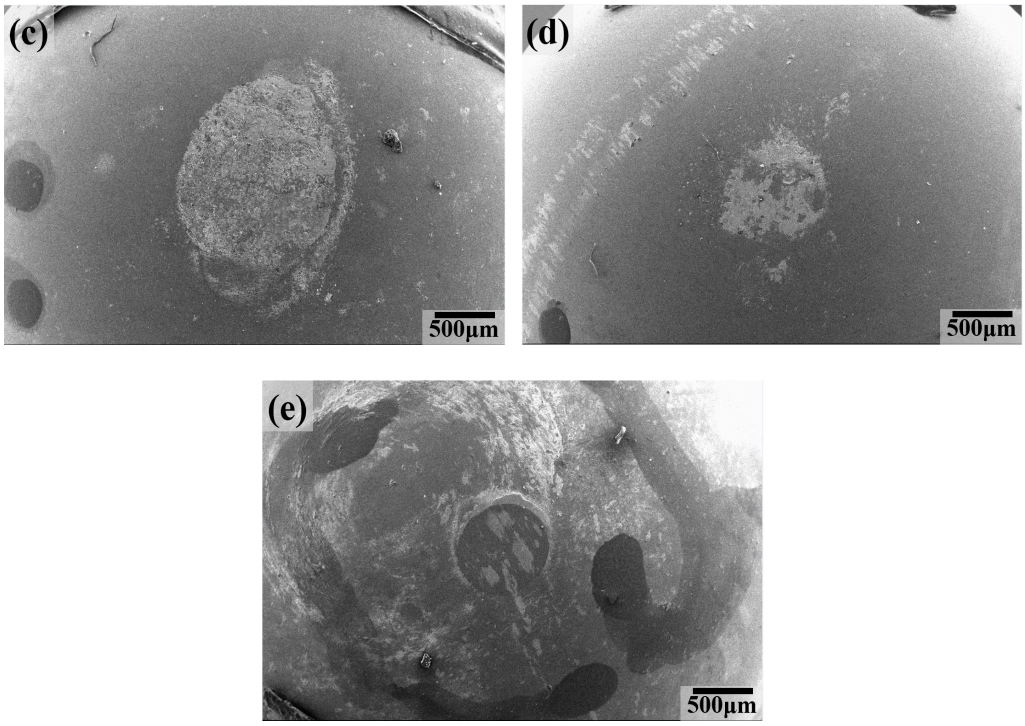


Figure 12. SEM images of the worn surface of the Si_3N_4 ceramic ball sliding against the NAB composite at different testing temperatures: (**a**) 25 °C, (**b**) 200 °C, (**c**) 400 °C, (**d**) 600 °C, and (**e**) 800 °C.

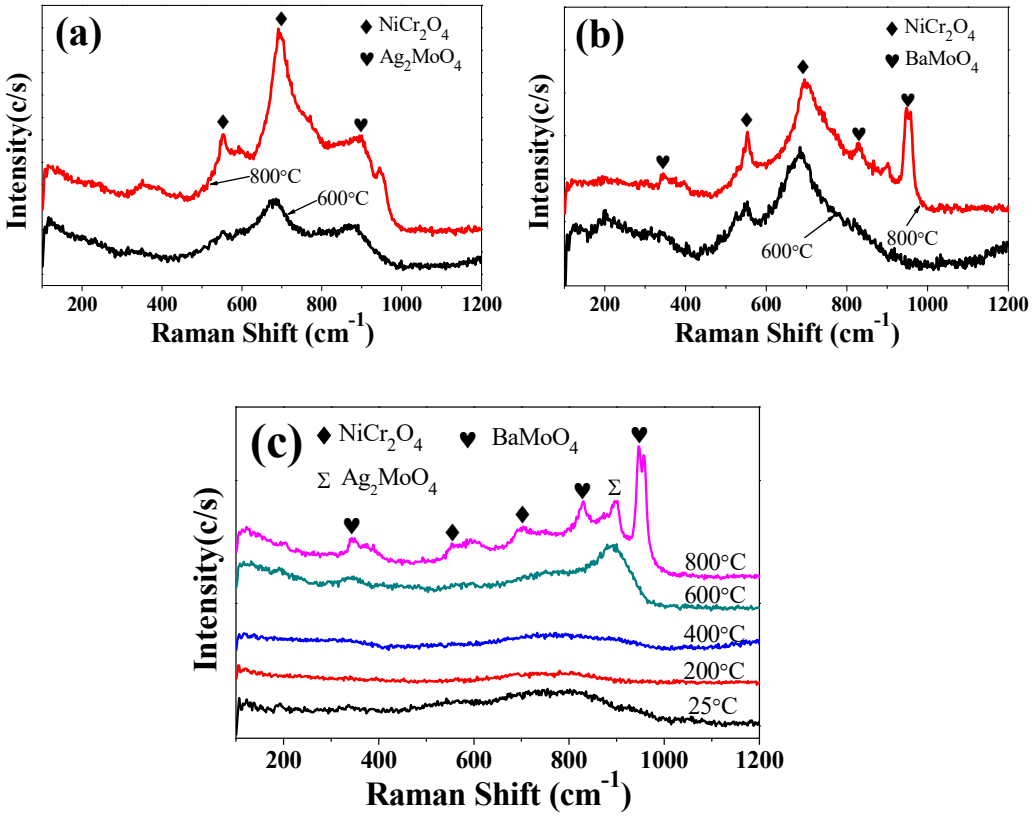


Figure 13. Raman spectrum of the worn surface for composites: (**a**) NA at 600 and 800 °C, (**b**) NB at 600 and 800 °C, and (**c**) NAB composites at 25, 200, 400, 600, and 800 °C.

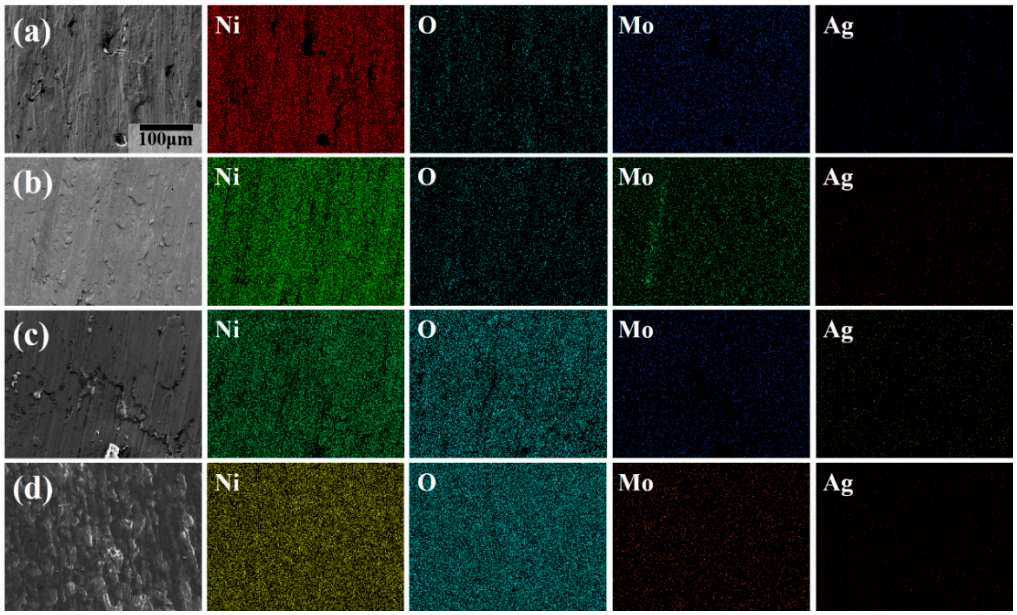


Figure 14. SEM images and the corresponding element distribution of the NA composite at different testing temperatures: (**a**) 25 °C, (**b**) 400 °C, (**c**) 600 °C, and (**d**) 800 °C.

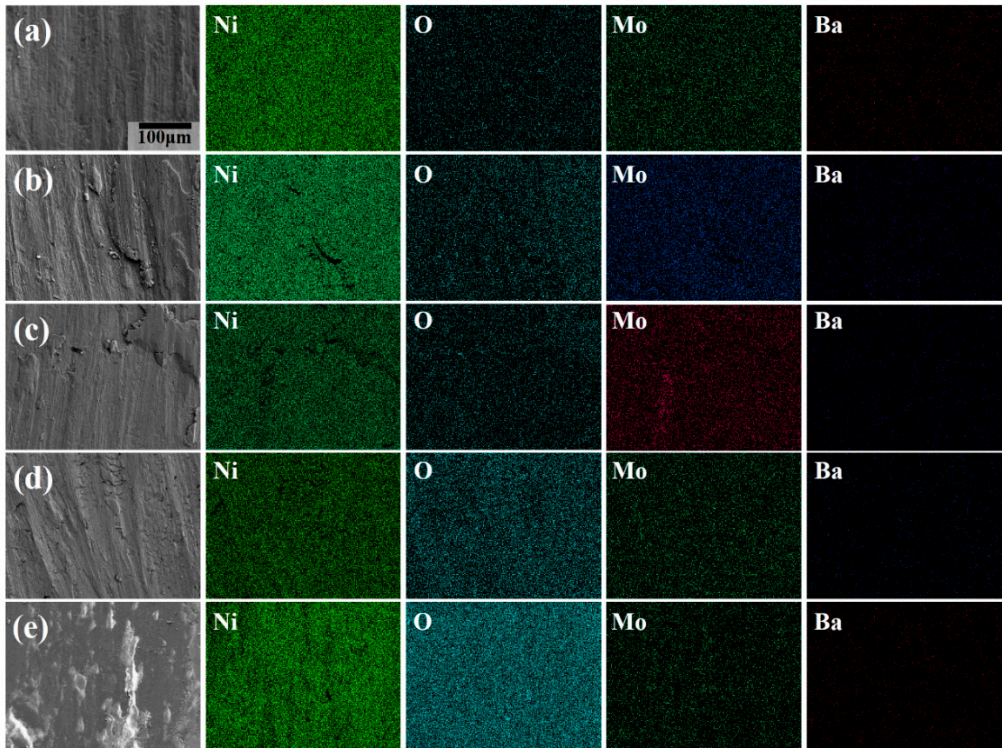


Figure 15. SEM images and the corresponding element distribution of the NB composite at different testing temperatures: (**a**) 25 °C, (**b**) 200 °C, (**c**) 400 °C, (**d**) 600 °C, and (**e**) 800 °C.

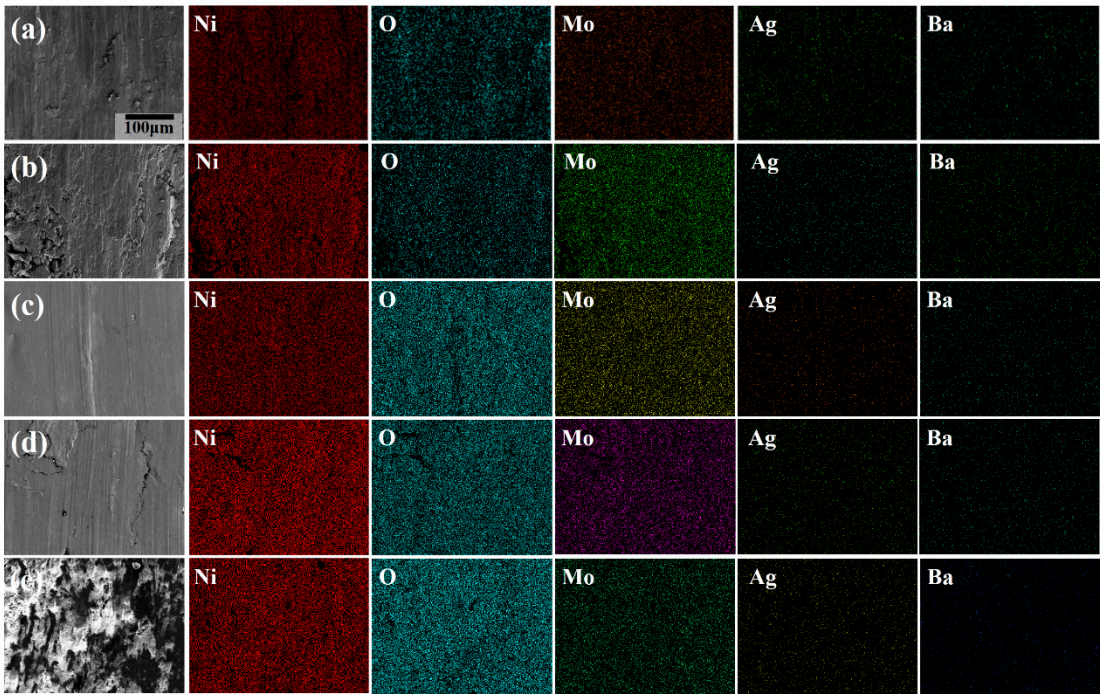


Figure 16. SEM images and the corresponding element distribution of the NAB composite at different testing temperatures: (**a**) 25 °C, (**b**) 200 °C, (**c**) 400 °C, (**d**) 600 °C, and (**e**) 800 °C.

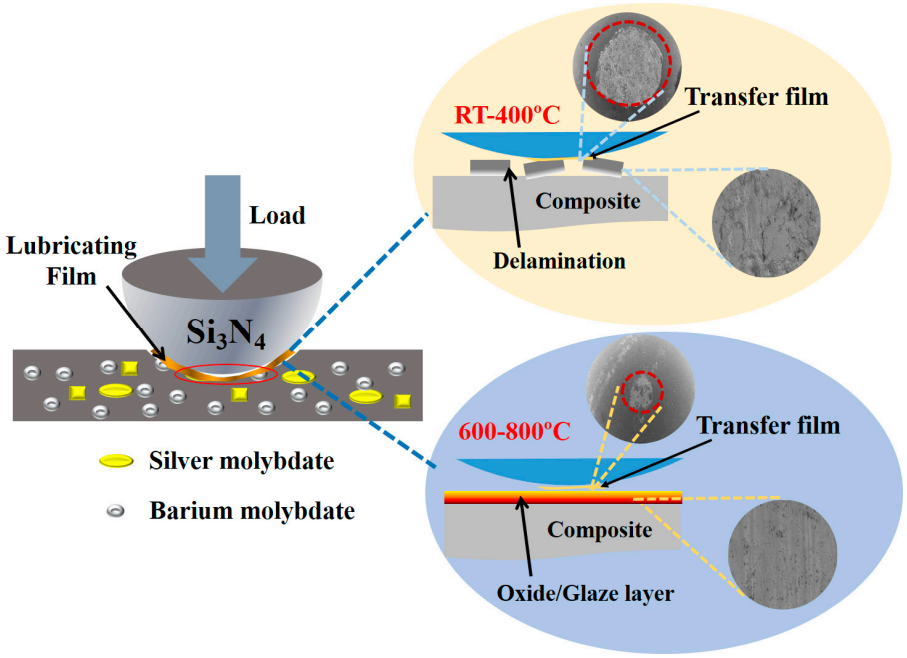


Figure 17. Schematic of the wear mechanism for composites at different testing temperatures.

4. Conclusions

The present study examined the preparation of nickel-alloy matrix composites incorporating Ag_2MoO_4 and $BaMoO_4$ by the hot-pressed sintering process. Subsequently, the tribological characteristics of these composites were examined within an air temperature range of 25 to 800 °C. The primary findings may be inferred as follows:

(1) Due to the lack of a low-temperature solid lubricant, all three composites showed poor lubricating performance at low testing temperatures. As the temperature increased

to 600 °C/800 °C, the in-situ-formed oxidative lubricating layer on the worn surface resulted in relatively low COFs and wear rates.

(2) The NB composite presents a relatively low wear rate of (1.75–4.59) $\times 10^{-4}$ $mm^3/N^{-1}m^{-1}$ from 25 to 800 °C. NAB composites show the best lubricating properties from 400 °C to 800 °C, and the COFs and wear rates are approximately 0.34–0.5 and (0.47–1.25) $\times 10^{-4}$ $mm^3/N^{-1}m^{-1}$.

(3) From 600 to 800 °C, the composites exhibit low friction and wear rates in comparison to their performance at lower temperatures. From 25 to 400 °C, during the sliding process, most of the lubricating film that formed on the sliding surface is removed, thus resulting in a relatively high COF and wear rate; the primary wear mechanisms under these conditions are severe abrasive and fatigue wear. Within the temperature range of 600 to 800 °C, the observed reduction in COF and wear rate may be attributed to the synergistic lubricating action of Ag_2MoO_4, $BaMoO_4$, and the in-situ-formed oxide. Thus, slightly abrasive wear is the dominant wear mechanism.

(4) It has been reported that the friction and wear behavior of counterpart materials are quite dependent on the transfer film, especially the increased thickness with sliding time. As a further investigation, we plan to study the thickness variation of the transfer film formed on the counterpart materials and its wear performance for the nickel-alloy matrix composite. The results of this project will provide theoretical guidance and technical support for the design and preparation of high-performance anti-wear materials, which are used in aerospace, nuclear powder, high-end equipment, and other sports power systems.

Author Contributions: Methodology, J.Z.; software, L.Y. (Liwei Yang); investigation, T.Y.; data curation, C.Z., Y.H., L.Y. (Lin Yuan), T.Y. and S.G.; writing—original draft preparation, C.Z. and J.Z.; writing—review and editing, J.Z. All authors have read and agreed to the published version of the manuscript.

Funding: This work was supported by the National Natural Science Foundation of China (52105190), the Guangyue Young Scholar Innovation Team of Liaocheng University (LCUGYTD2023-02), and the Liaocheng Small- and Medium-sized Enterprise Climbing Plans (2022PDJH25, 2022PDJH22).

Data Availability Statement: Data are contained within the article.

Conflicts of Interest: The authors declare no conflict of interest.

References

1. John, M.; Menezes, P.L. Self-lubricating materials for extreme condition applications. *Materials* **2021**, *14*, 5588. [CrossRef] [PubMed]
2. Zhu, S.; Cheng, J.; Qiao, Z.; Yang, J. High temperature solid-lubricating materials: A review. *Tribol. Int.* **2019**, *133*, 206–233. [CrossRef]
3. Ouyang, J.; Li, Y.; Zhang, Y.; Wang, Y.; Wang, Y. High-temperature solid lubricants and self-lubricating composites: A critical review. *Lubricants* **2022**, *10*, 177. [CrossRef]
4. Sliney, H.E. Solid lubricant materials for high temperatures—A review. *Tribol. Int.* **1982**, *15*, 303–315. [CrossRef]
5. Muratore, C.; Voevodin, A.A. Chameleon coatings: Adaptive surfaces to reduce friction and wear in extreme environments. *Annu. Rev. Mater. Res.* **2009**, *39*, 297–324. [CrossRef]
6. Zhen, J.; Han, Y.; Cheng, J.; Chen, W.; Yang, J.; Jia, Z.; Zhang, R. Enhancing the wide temperature dry sliding tribological performance of nickle-alloy by adding MoS_2/CaF_2. *Tribol. Int.* **2022**, *165*, 107254. [CrossRef]
7. Kostadinov, G.; Penyashki, T.; Elenov, B.; Danailov, P.; Dimitrova, R.; Kandeva, M.; Kamburov, V.; Nikolov, A. Surface topography and roughness parameters of electrospark coatings on titanium and nickel alloys. *Appl. Eng. Lett.* **2021**, *6*, 89–98. [CrossRef]
8. Bulei, C.; Stojanovic, B.; Utu, D. Developments of discontinuously reinforced aluminium matrix composites: Solving the needs for the matrix. *J. Phys. Conf. Ser.* **2022**, *2212*, 012029. [CrossRef]
9. Kong, X.; Sun, W.; Wang, Q.; Chen, M.; Zhang, T.; Wang, F. Improving high-temperature wear resistance of NiCr matrix self-lubricating composites by controlling oxidation and surface texturing. *J. Mater. Sci. Technol.* **2022**, *131*, 253–263. [CrossRef]
10. Kumar, R.; Antonov, M. Self-lubricating materials for extreme temperature tribo-applications. *Mater. Today Proc.* **2020**, *44*, 4583–4589. [CrossRef]
11. Zhu, S.; Bi, Q.; Yang, J.; Liu, W. Effect of fluoride content on friction and wear performance of Ni_3Al matrix high-temperature self-lubricating composites. *Tribol. Lett.* **2011**, *43*, 341–349. [CrossRef]

12. Zhu, S.; Bi, Q.; Yang, J.; Liu, W.; Xue, Q. Effect of particle size on tribological behavior of Ni_3Al matrix high temperature self-lubricating composites. *Tribol. Int.* **2011**, *44*, 1800–1809. [CrossRef]
13. Zhu, S.; Bi, Q.; Yang, J.; Liu, W.; Xue, Q. Ni_3Al matrix high temperature self-lubricating composites. *Tribol. Int.* **2011**, *44*, 445–453. [CrossRef]
14. Zhu, S.; Bi, Q.; Niu, M.; Yang, J.; Liu, W. Tribological behavior of NiAl matrix composites with addition of oxides at high temperatures. *Wear* **2012**, *274–275*, 423–434. [CrossRef]
15. Shi, X.; Wang, M.; Zhai, W.; Xu, Z.; Zhang, Q.; Chen, Y. Influence of Ti_3SiC_2 content on tribological properties of NiAl matrix self-lubricating composites. *Mater. Des.* **2013**, *45*, 179–189. [CrossRef]
16. Shi, X.; Song, S.; Zhai, W.; Wang, M.; Xu, Z.; Yao, J.; ud Din, A.Q.; Zhang, Q. Tribological behavior of Ni_3Al matrix self-lubricating composites containing WS_2, Ag and hBN tested from room temperature to 800 °C. *Mater. Des.* **2014**, *55*, 75–84. [CrossRef]
17. Shi, X.; Zhai, W.; Wang, M.; Xu, Z.; Yao, J.; Song, S.; Wang, Y. Tribological behaviors of NiAl based self-lubricating composites containing different solid lubricants at elevated temperatures. *Wear* **2014**, *310*, 1–11. [CrossRef]
18. Kumar, R.; Antonov, M.; Varga, M.; Hussainova, I.; Ripoll, M.R. Synergistic effect of Ag and MoS_2 on high-temperature tribology of self-lubricating NiCrBSi composite coatings by laser metal deposition. *Wear* **2023**, *532–533*, 205114. [CrossRef]
19. Sun, J.; Liu, C.; Venturi, F.; Romero, A.R.; Hussain, T. Dry sliding wear behaviour of suspension HVOF thermal sprayed Al_2O_3-MoS_2 and Al_2O_3-BN nanotube coatings. *J. Alloys Compd.* **2023**, *966*, 171582. [CrossRef]
20. Li, R.; Zhao, X.; Bu, Z.; An, Y.; Zhou, H.; Duan, W.; Chen, J. Influence of different introduction modes of metal Ag into plasma sprayed Al_2O_3 coating on tribological properties. *Ceram. Int.* **2022**, *48*, 9286–9296. [CrossRef]
21. Kong, L.; Bi, Q.; Zhu, S.; Yang, J.; Liu, W. Tribological properties of ZrO_2 (Y_2O_3)–Mo–BaF_2/CaF_2 composites at high temperatures. *Tribol. Int.* **2012**, *45*, 43–49. [CrossRef]
22. Kong, L.; Zhu, S.; Bi, Q.; Qiao, Z.; Yang, J.; Liu, W. Friction and wear behavior of self-lubricating $ZrO_2(Y_2O_3)$-CaF_2-Mo-graphite composite from 20 °C to 1000 °C. *Ceram. Int.* **2014**, *40*, 10787–10792. [CrossRef]
23. Kong, L.; Zhu, S.; Qiao, Z.; Yang, J.; Bi, Q.; Liu, W. Effect of Mo and Ag on the friction and wear behavior of ZrO_2 (Y_2O_3)–Ag–CaF_2–Mo composites from 20 °C to 1000 °C. *Tribol. Int.* **2014**, *78*, 7–13. [CrossRef]
24. Gao, H.; Otero-de-la-Roza, A.; Gu, J.; Stone, D.; Aouadi, S.M.; Johnson, E.R.; Martini, A. (Ag,Cu)-Ta-O ternaries as high-temperature solid-lubricant coatings. *ACS Appl. Mater. Interfaces* **2015**, *7*, 15422–15429. [CrossRef]
25. Stone, D.; Migas, J.; Martini, A.; Smith, T.; Muratore, C.; Voevodin, A.; Aouadi, S. Adaptive NbN/Ag coatings for high temperature tribological applications. *Surf. Coat. Technol.* **2012**, *206*, 4316–4321. [CrossRef]
26. Roy, A.; Patel, P.; Sharifi, N.; Chromik, R.; Stoyanov, P.; Moreau, C. Binary and ternary lubricious oxides for high temperature tribological applications: A review. *Results Surf. Interfaces* **2023**, *11*, 100117. [CrossRef]
27. Voevodin, A.A.; Muratore, C.; Aouadi, S.M. Hard coatings with high temperature adaptive lubrication and contact thermal management: Review. *Surf. Coat. Technol.* **2014**, *257*, 247–265. [CrossRef]
28. Wang, D.; Tan, H.; Chen, W.; Zhu, S.; Cheng, J.; Yang, J. Tribological behavior of Ni_3Al–Ag based self-lubricating alloy with Ag_2MoO_4 formed by high temperature tribo-chemical reaction. *Tribol. Int.* **2021**, *153*, 106659. [CrossRef]
29. Shi, P.; Yi, G.; Wan, S.; Sun, H.; Feng, X.; Pham, S.T.; Tieu, K.A.; Xie, E.; Wang, Q. High temperature tribological performance of nickel-based composite coatings by incorporating multiple oxides (TiO_2–ZnO–MoO_3). *Tribol. Int.* **2020**, *155*, 106759. [CrossRef]
30. Su, W.; Zhang, J.; Zhang, J.; Zhou, K.; Niu, S.; Liu, M.; Dai, H.; Deng, C. Microstructure of HVOF-sprayed Ag–BaF_2·CaF_2–Cr_3C_2–NiCr coating and its tribological behavior in a wide temperature range (25 °C to 800 °C). *Ceram. Int.* **2021**, *47*, 865–876. [CrossRef]
31. Yang, J.; Jia, J.; Li, X.; Lu, C.; Feng, X. Synergistic lubrication of Ag and Ag2MoO4 nanoparticles anchored in plasma-sprayed YSZ coatings: Remarkably-durable lubricating performance at 800 °C. *Tribol. Int.* **2021**, *153*, 106670. [CrossRef]
32. Zhen, J.; Cheng, J.; Li, M.; Zhu, S.; Long, Z.; Yang, B.; Yang, J. Lubricating behavior of adaptive nickel alloy matrix composites with multiple solid lubricants from 25 °C to 700 °C. *Tribol. Int.* **2017**, *109*, 174–181. [CrossRef]
33. Zhen, J.; Zhu, S.; Cheng, J.; Li, M.; Lu, Y.; Qiao, Z.; Yang, J. Influence of graphite content on the dry sliding behavior of nickel alloy matrix solid lubricant composites. *Tribol. Int.* **2017**, *114*, 322–328. [CrossRef]
34. Li, F.; Cheng, J.; Qiao, Z.; Ma, J.; Zhu, S.; Fu, L.; Yang, J.; Liu, W. A Nickel-Alloy-Based High-Temperature Self-Lubricating Composite with Simultaneously Superior Lubricity and High Strength. *Tribol. Lett.* **2013**, *49*, 573–577. [CrossRef]
35. Cheng, J.; Li, F.; Zhu, S.; Hao, J.; Yang, J.; Li, W.; Liu, W. High temperature tribological properties of a nickel-alloy-based solid-lubricating composite: Effect of surface tribo-chemistry, counterpart and mechanical properties. *Wear* **2017**, *386–387*, 39–48. [CrossRef]
36. Yao, Q.; Jia, J.; Chen, T.; Xin, H.; Shi, Y.; He, N.; Feng, X.; Shi, P.; Lu, C. High temperature tribological behaviors and wear mechanisms of NiAl-MoO_3/CuO composite coatings. *Surf. Coat. Technol.* **2020**, *395*, 125910. [CrossRef]
37. Aouadi, S.M.; Paudel, Y.; Simonson, W.J.; Ge, Q.; Kohli, P.; Muratore, C.; Voevodin, A.A. Tribological investigation of adaptive Mo_2N/MoS_2/Ag coatings with high sulfur content. *Surf. Coat. Technol.* **2009**, *203*, 1304–1309. [CrossRef]
38. Zhen, J.; Li, F.; Zhu, S.; Ma, J.; Qiao, Z.; Liu, W.; Yang, J. Friction and wear behavior of nickel-alloy-based high temperature self-lubricating composites against Si_3N_4 and Inconel 718. *Tribol. Int.* **2014**, *75*, 1–9. [CrossRef]
39. Lopes, F.; Noleto, L.; Vieira, V.; de Sousa, P.; Jucá, A.; Oliveira, Y.; Costa, K.; Almeida, M.; Gouveia, A.; Cavalcante, L. Experimental and theoretical correlation of modulated architectures of β-Ag_2MoO_4 microcrystals: Effect of different synthesis routes on the morphology, optical, colorimetric, and photocatalytic properties. *J. Inorg. Organomet. Polym. Mater.* **2023**, *33*, 424–450. [CrossRef]

40. Kumar, J.; Karthik, R.; Chen, S.; Muthuraj, V.; Karuppiah, C. Fabrication of potato-like silver molybdate microstructures for photocatalytic degradation of chronic toxicity ciprofloxacin and highly selective electrochemical detection of H_2O_2. *Sci. Rep.* **2016**, *6*, 34149. [CrossRef]
41. Jena, P.; Nallamuthu, N.; Hari Prasad, K.; Venkateswarlu, M.; Satyanarayana, N. Structural characterization and electrical conductivity studies of $BaMoO_4$ nanofibers prepared by sol–gel and electrospinning techniques. *J. Sol-Gel Sci. Technol.* **2014**, *72*, 480–489. [CrossRef]

Disclaimer/Publisher's Note: The statements, opinions and data contained in all publications are solely those of the individual author(s) and contributor(s) and not of MDPI and/or the editor(s). MDPI and/or the editor(s) disclaim responsibility for any injury to people or property resulting from any ideas, methods, instructions or products referred to in the content.